http://dx.doi.org/10.11142/jicems.2014.3.3.289
Journal of International Conference on Electrical Machines and Systems vol. 3, no. 3, pp. 289~297, 2014

Sensorless IPMSM Drives based on Extended Nonlinear State Observer with Parameter Inaccuracy Compensation

Yongle Mao*, Guiying Liu and Yangsheng Chen*****

Abstract – This paper proposed a novel high performance sensorless control scheme for IPMSM based on an extended nonlinear state observer. The gain-matrix of the observer has been derived by using state linearization method. Steady state errors in estimated rotor position and speed due to parameter inaccuracy have been analyzed, and an equivalent flux error is defined to represent the overall effect of parameter errors contributing to the wrong convergence of the estimated rotor speed as well as rotor position. Then, an online compensation strategy was proposed to limit the estimation errors in rotor position and speed. The effectiveness of the extended nonlinear state observer is validated through simulation and experimental test.

Keywords: IPMSM, Load Torque Estimation, Nonlinear State Observer, Parameter Inaccuracy Compensation, Sensorless Control

1. Introduction

Various model-based sensorless control schemes have been proposed for PM (Permanent Magnet) synchronous motors to replace the mechanical position sensor which is indispensible in a Field-Oriented-Control system [1-10]. Among them, the nonlinear state observer method for SPMSM (Surface Permanent Magnet Synchronous Motor), based on state linearization strategy, is superior for its outstanding dynamic performance and wide operating speed range [1-2]. It has been expanded to IPMSM (Interior Permanent Magnet Synchronous Motor) system by G. Bisheimer [3] and B. S. Bhangu [4], considering the physical back EMF only in deriving observer gain matrix. Steady state errors can be observed due to the lack of load torque estimation.

The major obstacle in applying model-based sensorless control strategies to IPMSM is the position dependent inductance matrix owing to the inductance difference between d- and q- axis. The concept of extended back EMF is first introduced by Z. Q. Chen to solve the problem [5]. Then, a group of more concise models are proposed primarily for flux linkage based sensorless control methods [6-8], in which the derivative of d- axis current generated in mathematical manipulation is not an issue.

It is believed that precise estimation for rotor position and speed requires the knowledge of accurate motor parameters. Unfortunately, all parameters of IPMSM tend to vary with different operating conditions. For example, inductances of d- and q- axis change with the level of magnetic saturation [12], while stator resistance and PM flux linkage depend on motor temperature. In [9], the impact of inaccurate parameters and inverter nonlinearity on the estimation of rotor position is investigated, and an estimation error equation has been derived, but the impact of erroneously estimated rotor speed is not investigated. It has been demonstrated in [10] that simultaneously estimation of rotor speed and identification of PM flux linkage based on MRAS (Model Reference Adaptive System) may cause incorrect convergence due to rank-deficient problem. Although RLS (Recursive Least-Square) method is capable of realizing online identification of multiple parameters [11], the algorithm is too complex to be implemented in practice.

In this paper, a synthetic back EMF is defined to transform IPMSM into SPMSM combining feedback linearization method. Then an extended nonlinear state observer is constructed in the stator-fixed coordinate frame based on state linearization method. The steady state error equations of the estimated rotor position and speed due to parameter inaccuracy are derived in the rotor-fixed

* Department of Electrical Engineering, Zhejiang University, China. (maoyongle@zju.edu.cn)
** College of Physics and Electronic Engineering, Guangxi Teachers Education University, China. (liugy78@163.com)
*** Department of Electrical Engineering, Zhejiang University, China. (yschen@zju.edu.cn)
Received 28 July 2014; Accepted 02 Aug 2014

coordinate frame, and an online compensation strategy is proposed to achieve high performance speed control of IPMSM system over wide speed range.

2. EXTENDED NONLINEAR STATE OBSERVER

2.1 Mathematical Model

The voltage equation of IPMSM in αβ frame is

$$\begin{pmatrix} u_\alpha \\ u_\beta \end{pmatrix} = R_s \begin{pmatrix} i_\alpha \\ i_\beta \end{pmatrix} + \mathrm{p}L_0 \begin{pmatrix} i_\alpha \\ i_\beta \end{pmatrix} + P\omega_m \psi_f \begin{pmatrix} -\sin\theta_e \\ \cos\theta_e \end{pmatrix} + \begin{pmatrix} \eta_\alpha \\ \eta_\beta \end{pmatrix} \quad (1)$$

$$\boldsymbol{\eta} = \begin{pmatrix} \eta_\alpha \\ \eta_\beta \end{pmatrix} = \mathrm{p} \begin{pmatrix} L_0 \cos 2\theta_e & L_1 \sin 2\theta_e \\ L_1 \sin 2\theta_e & -L_0 \cos 2\theta_e \end{pmatrix} \begin{pmatrix} i_\alpha \\ i_\beta \end{pmatrix} \quad (2)$$

where

$$L_0 = (L_d + L_q)/2, \quad L_1 = (L_d - L_q)/2$$

u_α, u_β, i_α, i_β are stator voltages and currents in αβ frame. R_s and ψ_f are stator resistance and PM flux linkage. L_0 is the mean stator inductance, while L_1 is the differential stator inductance. L_d and L_q are inductances in dq frame. ω_m, θ_e and P are mechanical angular speed, electrical angular position and pole pairs respectively. p stands for the differential operator.

$$\begin{aligned} \boldsymbol{\eta} &= \begin{pmatrix} \mathrm{p}(L_1(-2\sin\theta_e \sin\theta_e + 1)i_\alpha) + \mathrm{p}(2L_1 \sin\theta_e \cos\theta_e i_\beta) \\ \mathrm{p}(2L_1 \sin\theta_e \cos\theta_e i_\alpha) - \mathrm{p}(L_1(2\cos\theta_e \cos\theta_e - 1)i_\beta) \end{pmatrix} \\ &= \begin{pmatrix} \mathrm{p}L_1 & 0 \\ 0 & \mathrm{p}L_1 \end{pmatrix} \begin{pmatrix} i_\alpha \\ i_\beta \end{pmatrix} + 2P\omega_m L_1 i_q \begin{pmatrix} \cos\theta_e \\ \sin\theta_e \end{pmatrix} - 2L_1 \dot{i}_q \begin{pmatrix} -\sin\theta_e \\ \cos\theta_e \end{pmatrix} \end{aligned} \quad (3)$$

An alternative transformation of (2) is also feasible with d-axis current i_d and its derivative $\dot{i}_d$.

$$\begin{aligned} \boldsymbol{\eta} &= \begin{pmatrix} \mathrm{p}(L_1(2\cos\theta_e \cos\theta_e - 1)i_\alpha) + \mathrm{p}(2L_1 \sin\theta_e \cos\theta_e i_\beta) \\ \mathrm{p}(2L_1 \sin\theta_e \cos\theta_e i_\alpha) - \mathrm{p}(L_1(2\sin\theta_e \sin\theta_e - 1)i_\beta) \end{pmatrix} \\ &= \begin{pmatrix} -\mathrm{p}L_1 & 0 \\ 0 & -\mathrm{p}L_1 \end{pmatrix} \begin{pmatrix} i_\alpha \\ i_\beta \end{pmatrix} + 2P\omega_m L_1 i_d \begin{pmatrix} -\sin\theta_e \\ \cos\theta_e \end{pmatrix} + 2L_1 \dot{i}_d \begin{pmatrix} \cos\theta_e \\ \sin\theta_e \end{pmatrix} \end{aligned} \quad (4)$$

(2) contains a position dependent inductance matrix, which is inconvenient in applying nonlinear state observer method to IPMSM. This problem can be solved with appropriate mathematical manipulations [5-8]. A valid transformation of (2) is obtained employing q-axis current i_q and its derivative $\dot{i}_q$.

It can be seen that the position dependent inductance matrix is disappeared in both of the transformations given in (3) and (4). The transformation used in [4] is identical to that in (3) and is limited to IPMSMs with small saliency [5], for vector **B** defined in (3) is orthogonal to physical back EMF $\mathbf{E}_0$ as illustrated in Fig. 1 (a), and only $\mathbf{E}_0$ could be utilized in deriving the gain matrix of the nonlinear state observer.

As depicted in Fig. 1 (b), vector **D** defined in (4) is aligned with $\mathbf{E}_0$, which makes the transformation in (4) more suitable on the stage of state linearization. And a synthetic back EMF $\mathbf{E}_{syn}$ is defined directly by synthesizing **D** and $\mathbf{E}_0$ as given in (5). It is worth mentioning that the synthetic back EMF is essentially different from those concepts defined as flux linkages which are intended for sensorless control systems based on flux linkage primarily, such as fictitious flux [6] and linear flux [7], as well as equivalent back EMF [8], which is the derivative of a composite flux linkage by neglecting $\dot{i}_d$.

$$\mathbf{E}_{syn} = P\omega_m(\psi_f + 2L_1 i_d) \begin{pmatrix} -\sin\theta_e \\ \cos\theta_e \end{pmatrix} \quad (5)$$

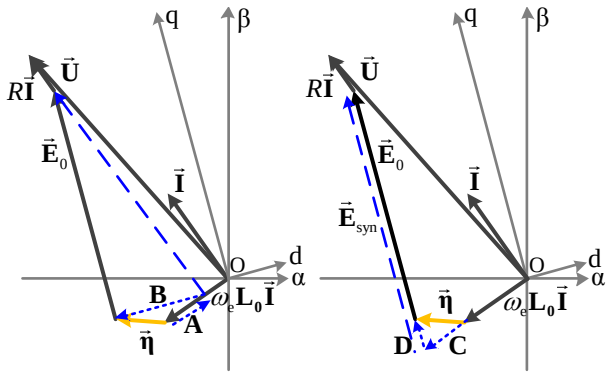

(a) Corresponding to (3) (b) Corresponding to (4)

Fig. 1. Phasor diagrams of IPMSM under steady state condition.

Compared with typical voltage equation of SPMSM in αβ frame, there is still an accessory voltage component orthogonal to $\mathbf{E}_0$, which is relating to the derivative of d-axis current. As the slope of d-axis reference current is limited, it is reasonable to introduce an auxiliary input υ, according feedback linearization method proposed in [13].

$$\boldsymbol{\upsilon}=\begin{pmatrix}\upsilon_\alpha\\ \upsilon_\beta\end{pmatrix}=\begin{pmatrix}u_\alpha-2L_1\dot{i}_\mathrm{d}\cos\theta_\mathrm{e}\\ u_\beta-2L_1\dot{i}_\mathrm{d}\sin\theta_\mathrm{e}\end{pmatrix} \tag{6}$$

Based on the synthetic back EMF $\mathbf{E}_{\mathrm{syn}}$ and auxiliary input $\boldsymbol{\upsilon}$, the voltage equation of IPMSM is reorganized as (7), which is equivalent to that of SPMSM.

$$\begin{pmatrix}\upsilon_\alpha\\ \upsilon_\beta\end{pmatrix}=R_\mathrm{s}\begin{pmatrix}i_\alpha\\ i_\beta\end{pmatrix}+\mathrm{p}L_\mathrm{q}\begin{pmatrix}i_\alpha\\ i_\beta\end{pmatrix}+P\omega_\mathrm{m}\psi_{\mathrm{syn}}\begin{pmatrix}-\sin\theta_\mathrm{e}\\ \cos\theta_\mathrm{e}\end{pmatrix} \tag{7}$$

where

$$\psi_{\mathrm{syn}}=(\psi_\mathrm{f}+2L_1i_\mathrm{d})$$

2.2 Extended Nonlinear State Observer

The mechanical equation of IPMSM system is expressed as

$$\begin{pmatrix}J\mathrm{p}\omega_\mathrm{m}\\ \mathrm{p}\theta_\mathrm{e}\end{pmatrix}=\begin{pmatrix}-B & 0\\ P & 0\end{pmatrix}\begin{pmatrix}\omega_\mathrm{m}\\ \theta_\mathrm{e}\end{pmatrix}+\begin{pmatrix}T_\mathrm{e}-T_\mathrm{L}\\ 0\end{pmatrix} \tag{8}$$

where

$$T_\mathrm{e}=1.5P\psi_{\mathrm{syn}}i_\mathrm{q}/J$$

J and B are the inertia and friction coefficient of mechanical system respectively. T_e is the electromagnetic torque, while T_L is the load torque imposed on motor shaft, and is unknown in general.

Combining voltage equation (7) and mechanical equation (8), as well as the dynamic equation of load torque, the overall state equations of IPMSM are given as

$$\begin{cases}\dot{\mathbf{x}}=\mathrm{f}(\mathbf{x})\\ \mathbf{y}=\mathrm{h}(\mathbf{x})\end{cases} \tag{9}$$

where $\mathbf{x}$ and $\mathbf{y}$ are system input and out vectors.

$$x=\begin{pmatrix}i_\alpha & i_\beta & \omega_\mathrm{m} & \theta_\mathrm{e} & T_\mathrm{L}\end{pmatrix}^\mathrm{T}$$

$$\mathrm{f}(x)=\begin{pmatrix}\dfrac{-R_\mathrm{s}}{L_\mathrm{q}}i_\alpha+\dfrac{\psi_{\mathrm{syn}}}{L_\mathrm{q}}P\omega_\mathrm{m}\sin\theta_\mathrm{e}+\dfrac{\upsilon_\alpha}{L_\mathrm{q}}\\ \dfrac{-R_\mathrm{s}}{L_\mathrm{q}}i_\beta-\dfrac{\psi_{\mathrm{syn}}}{L_\mathrm{q}}P\omega_\mathrm{m}\cos\theta_\mathrm{e}+\dfrac{\upsilon_\beta}{L_\mathrm{q}}\\ \dfrac{1.5P\psi_{\mathrm{syn}}i_\mathrm{q}}{J}-\dfrac{B}{J}\omega_\mathrm{m}-\dfrac{T_\mathrm{L}}{J}\\ P\omega_\mathrm{m}\\ 0\end{pmatrix}$$

Although a null-load assumption will not affect the observer's asymptotic stability, estimation errors may arise due to the unstructured uncertainties. Compared with electrical time constant, load torque can be assumed to be constant in a sampling period, which means $T_\mathrm{L}/dt\approx 0$. And it can be added as an extended state in the state equations of IPMSM system [2].

$$\mathrm{h}(x)=\begin{pmatrix}i_\alpha & 0 & 0 & 0 & 0\\ 0 & i_\beta & 0 & 0 & 0\end{pmatrix}$$

To investigate the observability of (9), it is necessary to recall the definition of Lie derivative [14-15], as shown bellow

$$\begin{cases}\mathrm{L_f}\,\mathrm{h}(x)=\nabla\mathrm{h}(x)\,\mathrm{f}(x)\\ \mathrm{L_f^k}\,\mathrm{h}(x)=\mathrm{L_f}\left(\mathrm{L_f^{k-1}}\,\mathrm{h}(x)\right)\end{cases} \tag{10}$$

where ∇ represents the gradient operator and $\mathrm{L_f^k}\,\mathrm{h}(x)$ means k times of iteration of $\mathrm{L_f}\,\mathrm{h}(x)$.

Substituting (10) to (9) yields

$$\nabla\mathrm{h}(x)=\frac{\partial}{\partial x}\mathrm{h}(x)=\begin{pmatrix}1 & 0 & 0 & 0 & 0\\ 0 & 1 & 0 & 0 & 0\end{pmatrix} \tag{11}$$

$$\mathrm{L_f}\,\mathrm{h}(x)=\nabla\mathrm{h}(x)\,\mathrm{f}(x)=\begin{pmatrix}-c_1i_\alpha+c_2P\omega_\mathrm{m}\sin\theta_\mathrm{e}+\upsilon_\alpha/L_\mathrm{q}\\ -c_1i_\beta-c_2P\omega_\mathrm{m}\cos\theta_\mathrm{e}+\upsilon_\beta/L_\mathrm{q}\end{pmatrix} \tag{12}$$

$$\mathrm{L_f^2}\,\mathrm{h}(x)=\begin{pmatrix}\sigma_1(i_\alpha,i_\beta,\omega_\mathrm{m},\theta_\mathrm{e})-c_2c_4P\sin\theta_\mathrm{e}T_\mathrm{L}\\ \sigma_2(i_\alpha,i_\beta,\omega_\mathrm{m},\theta_\mathrm{e})+c_2c_4P\cos\theta_\mathrm{e}T_\mathrm{L}\end{pmatrix} \tag{13}$$

$$\frac{\partial}{\partial x}\left(\mathrm{L_f^2}\,\mathrm{h}(x)\right)=\begin{pmatrix}* & * & * & * & -c_2c_4P\sin\theta_\mathrm{e}\\ * & * & * & * & c_2c_4P\cos\theta_\mathrm{e}\end{pmatrix} \tag{14}$$

The observability matrix is obtained combining (11) to (14).

$$\mathrm{O}=\begin{pmatrix}1 & 0 & 0 & 0 & 0\\ 0 & 1 & 0 & 0 & 0\\ -c_1 & 0 & c_2\sin\theta_\mathrm{e} & c_2P\omega_\mathrm{m}^2\cos\theta_\mathrm{e} & 0\\ 0 & -c_1 & -c_2\cos\theta_\mathrm{e} & c_2P\omega_\mathrm{m}^2\sin\theta_\mathrm{e} & 0\\ * & * & * & * & -c_2c_4\sin\theta_\mathrm{e}\end{pmatrix} \tag{15}$$

where $c_1=R_\mathrm{s}/L_\mathrm{q}$, $c_2=\psi_{\mathrm{syn}}/L_\mathrm{q}$, $c_3=B/J$, $c_4=1/J$. And '*' denotes a non-zero term depending on motor parameters.

It is clear that the observability matrix is full rank and system (9) is locally observable except for $\omega_m = 0$.

The state linearization method, similar to that applied to SPMSM [1-2], is utilized in deriving the gain matrix of the extended nonlinear observer for IPMSM. The structure of gain matrix is determined in polar coordinate frame employing the coordinate transformation given in (16). To avoid ambiguity in the sign of the estimated rotor speed, a reverse transformation is complemented, as shown in (17), and the ultimate expression of the extended nonlinear state observer built in αβ frame is given in (18).

$$\begin{pmatrix} z_1 \\ z_2 \end{pmatrix} = \Phi(\omega_m, \theta_e) = \begin{pmatrix} \psi_{syn} P \omega_m \sin\theta_e / L_q \\ -\psi_{syn} P \omega_m \cos\theta_e / L_q \end{pmatrix} \tag{16}$$

$$\begin{pmatrix} \omega_m \\ \theta_e \end{pmatrix} = \Phi^{-1}(z_1, z_2) = \begin{pmatrix} L_q \sqrt{z_1^2 + z_2^2} \Big/ P\psi_{syn} \\ \arctan\left(-\dfrac{z_1}{z_2}\right) \Big/ P \end{pmatrix} \tag{17}$$

$$\frac{d}{dt}\begin{pmatrix} \hat{i}_\alpha \\ \hat{i}_\beta \\ \hat{\omega}_m \\ \hat{\theta}_e \\ \hat{T}_L \end{pmatrix} = \begin{pmatrix} \dfrac{-\hat{R}_s}{\hat{L}_q}\hat{i}_\alpha + \dfrac{\hat{\psi}_{syn}}{\hat{L}_q} P\hat{\omega}_m \sin\hat{\theta}_e + \dfrac{\upsilon'_\alpha}{\hat{L}_q} \\ \dfrac{-\hat{R}_s}{\hat{L}_q}\hat{i}_\beta - \dfrac{\hat{\psi}_{syn}}{\hat{L}_q} P\hat{\omega}_m \cos\hat{\theta}_e + \dfrac{\upsilon'_\beta}{\hat{L}_q} \\ \dfrac{1.5P\hat{\psi}_{syn} i_q}{J} - \dfrac{B}{J}\hat{\omega}_m - \dfrac{\hat{T}_L}{J} \\ P\hat{\omega}_m \\ 0 \end{pmatrix} + \mathbf{K}\begin{pmatrix} i_\alpha - \hat{i}_\alpha \\ i_\beta - \hat{i}_\beta \end{pmatrix} \tag{18}$$

where

$$\begin{cases} \upsilon'_\alpha = u_\alpha - (\hat{L}_d - \hat{L}_q)\dot{i}_d \cos\hat{\theta}_e \\ \upsilon'_\beta = u_\beta - (\hat{L}_d - \hat{L}_q)\dot{i}_d \sin\hat{\theta}_e \end{cases}$$

$$\mathbf{K} = \begin{pmatrix} K_y & 0 \\ 0 & K_y \\ \dfrac{K_\lambda L_q}{\psi_{syn}}\sin\hat{\theta}_e & -\dfrac{K_\lambda L_q}{\psi_{syn}}\cos\hat{\theta}_e \\ \dfrac{K_\lambda L_q}{P\hat{\omega}_m\psi_{syn}}\cos\hat{\theta}_e & \dfrac{K_\lambda L_q}{P\hat{\omega}_m\psi_{syn}}\sin\hat{\theta}_e \\ -K_t \sin\hat{\theta}_e & K_t \cos\hat{\theta}_e \end{pmatrix}$$

Variables with '^' represent the estimated values, while parameters with '^' stands for the measured values used in the observer.

2.3 Simulation Studies

The performance of the extended nonlinear state observer with accurate parameters is investigated through simulation, as shown in Fig. 2. The specifications of IPMSM are given in Table I. It can be seen that the dynamic performance of the extended nonlinear state observer is excellent, and nearly zero steady state errors in the estimated rotor position and speed are obtained by incorporating the estimation of load torque. In reality, the parameters of IPMSM tend to vary with different operating conditions. Parameters with '~' indicate the uncertainties in motor parameters, which are defined as

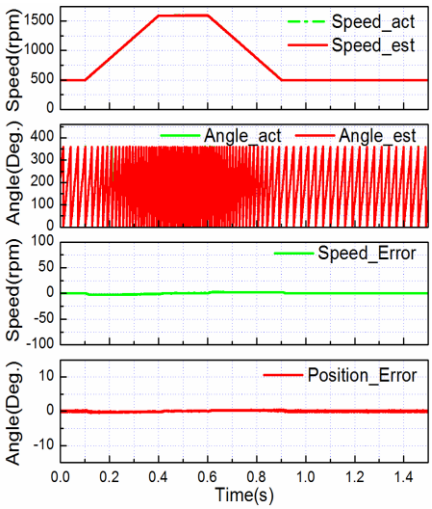

Fig. 2. Simulated performance of the extended nonlinear state observer with accurate parameters.

$$\begin{cases} \tilde{L}_q = L_q - \hat{L}_q, \tilde{L}_d = L_d - \hat{L}_d, \tilde{R}_s = R_s - \hat{R}_s \\ \tilde{\psi}_{syn} = \psi_f + (L_d - L_q)i_d - \hat{\psi}_f - (\hat{L}_d - \hat{L}_q)i_d \\ \quad = \tilde{\psi}_f + (\tilde{L}_d - \tilde{L}_q)i_d \end{cases} \tag{19}$$

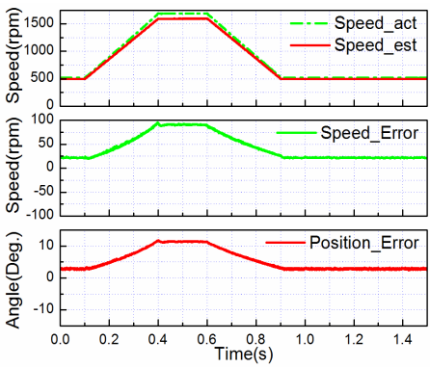

Fig. 3. Simulated performance of the extended nonlinear state observer with inaccurate parameters.

Simulation results in Fig. 3 show the performance of the extended nonlinear state observer with inaccurate parameters. In the observer, $\hat{R}_s$ is 85% of R_s, and $\hat{\psi}_f$ 105% of ψ_f, $\hat{L}_d$ 90% of L_d, $\hat{L}_q$ 110% of L_q, which are typical conditions in practice, because of motor heating and saturation effects. Although the observer is still stable, large steady state errors in estimated rotor position and speed can be observed, which varies with rotor speed.

3. Estimation errors

3.1 Impact of Parameter inaccuracy

Estimation errors in rotor position and speed are defined as

$$\tilde{\theta}_e = \theta_e - \hat{\theta}_e , \quad \tilde{\omega}_m = \omega_m - \hat{\omega}_m$$

Transforming (7) to the estimated dq frame gives

$$\begin{aligned}\begin{pmatrix} u_d \\ u_q \end{pmatrix} &= L_q \begin{pmatrix} \dot{i}_d \\ \dot{i}_q \end{pmatrix} + \begin{pmatrix} R_s & -P\omega_m L_q \\ P\omega_m L_q & R_s \end{pmatrix} \begin{pmatrix} i_d \\ i_q \end{pmatrix} \\ &+ \begin{pmatrix} 2L_1 \dot{i}_d \cos\tilde{\theta}_e - P\omega_m \psi_{syn} \sin\tilde{\theta}_e \\ 2L_1 \dot{i}_d \sin\tilde{\theta}_e + P\omega_m \psi_{syn} \cos\tilde{\theta}_e \end{pmatrix}\end{aligned} \tag{20}$$

The extended nonlinear state observer is separated and rewritten in the estimated dq frame as

$$\begin{aligned}\begin{pmatrix} u_d \\ u_q \end{pmatrix} &= \hat{L}_q \begin{pmatrix} \dot{\hat{i}}_d \\ \dot{\hat{i}}_q \end{pmatrix} + \begin{pmatrix} \hat{R}_s & -P\omega_m \hat{L}_q \\ P\omega_m \hat{L}_q & \hat{R}_s \end{pmatrix} \begin{pmatrix} \hat{i}_d \\ \hat{i}_q \end{pmatrix} \\ &+ \begin{pmatrix} 2\hat{L}_1 \dot{i}_d \\ P\hat{\omega}_m \hat{\psi}_{syn} \end{pmatrix} + \begin{pmatrix} K_y \hat{L}_q (i_d - \hat{i}_d) \\ K_y \hat{L}_q (i_q - \hat{i}_q) \end{pmatrix}\end{aligned} \tag{21}$$

$$\frac{d}{dt}\begin{pmatrix} J\hat{\omega}_m \\ \hat{\theta}_e \\ \hat{T}_L \end{pmatrix} = \begin{pmatrix} 1.5P\hat{\psi}_{syn} i_q - B\hat{\omega}_m - \hat{T}_L \\ P\hat{\omega}_m \\ 0 \end{pmatrix} + \begin{pmatrix} K_\lambda L_q (i_q - \hat{i}_q)/\psi_{syn} \\ K_\lambda L_q (i_d - \hat{i}_d)/P\hat{\omega}_m \psi_{syn} \\ -K_t (i_q - \hat{i}_q) \end{pmatrix} \tag{22}$$

Taking into account that high observer gains are necessary in order to stabilize the overall closed loop sensorless control system [1, 4] and the estimated load torque is adjusted by error between i_q and $\hat{i}_q$, the following approximations are made under steady state conditions:

1) $\hat{i}_d \approx i_d$, $\hat{i}_q = i_q$.

2) $\tilde{\theta}_e$ is sufficiently small, and $\sin\tilde{\theta}_e \approx \tilde{\theta}_e$, $\cos\tilde{\theta}_e \approx 1$.

3) $d\hat{\omega}_m/dt \approx 0$ and $d\hat{\theta}_e/dt \approx P\omega_m$.

With the above assumptions, the steady state error equations are obtained by subtracting (20) with (21) and rearranged as

$$\begin{cases} \tilde{R}_s i_d - P\omega_m \tilde{L}_q i_q - P\omega_m \psi_{syn} \tilde{\theta}_e = -(K_y \hat{L}_q + \hat{R}_s)(i_d - \hat{i}_d) \\ \tilde{R}_s i_q + P\omega_m (\tilde{\psi}_{syn} + \tilde{L}_q i_d) + P\tilde{\omega}_m \hat{\psi}_{syn} = -(K_y \hat{L}_q + \hat{R}_s)(i_q - \hat{i}_q) \end{cases} \tag{23}$$

Substituting (23) into (22) gives

$$\begin{cases} \dfrac{K_\lambda \hat{L}_q}{(K_y \hat{L}_q + \hat{R}_s)} \dfrac{\tilde{R}_s i_q + P\omega_m i_d \tilde{L}_q + P\omega_m \tilde{\psi}_{syn} + P\tilde{\omega}_m \hat{\psi}_{syn}}{\hat{\psi}_{syn}} \approx 0 \\ P\hat{\omega}_m - \dfrac{K_\lambda \hat{L}_q}{(K_y \hat{L}_q + \hat{R}_s)} \dfrac{\tilde{R}_s i_d - P\omega_m i_q \tilde{L}_q - P\omega_m \psi_{syn} \tilde{\theta}_e}{P\hat{\omega}_m \hat{\psi}_{syn}} \approx P\omega_m \end{cases} \tag{24}$$

Steady state errors in the estimated rotor position and speed are derived as

$$\tilde{\omega}_m = -\frac{\tilde{R}_s i_q + P\omega_m i_d \tilde{L}_q + P\omega_m \tilde{\psi}_{syn}}{P\hat{\psi}_{syn}} = -\frac{\omega_m \tilde{\psi}_f'}{\hat{\psi}_{syn}} \tag{25}$$

$$\begin{aligned}\tilde{\theta}_e &= \frac{\tilde{R}_s i_d - P\omega_m i_q \tilde{L}_q}{P\omega_m \psi_{syn}} + \frac{(K_y \hat{L}_q + \hat{R}_s) P\hat{\omega}_m \hat{\psi}_{syn}}{K_\lambda \hat{L}_q \omega_m \psi_{syn}} \tilde{\omega}_m \\ &= \frac{\tilde{R}_s i_d - P\omega_m i_q \tilde{L}_q}{P\omega_m \psi_{syn}} - \frac{(K_y \hat{L}_q + \hat{R}_s) P\hat{\omega}_m}{K_\lambda \hat{L}_q \psi_{syn}} \tilde{\psi}_f'\end{aligned} \tag{26}$$

where the equivalent flux error is defined as

$$\tilde{\psi}_f' = \tilde{\psi}_f + i_d \tilde{L}_d + \tilde{R}_s i_q / P\omega_m \tag{27}$$

Conclusions can be drawn as follows:

1) If all parameters are accurate, the estimated rotor position and speed will converge to their actual values, as shown in simulation results of Fig. 2.

2) Error in the estimated rotor position caused by erroneously estimated speed can be dominant in high speed range as shown in (26) and the simulation results of Fig. 3. Although it can be mitigated when a higher observer gain is applied, the effect is limited by observer stability conditions.

3) Uncertainties in L_d and R_s can be incorporated into the equivalent flux error, which will lead to speed estimation error.

3.2 Online Compensation Strategy

Measures should be taken to compensate for the impact of parameter inaccuracy, especially the uncertainty in PM flux linkage, whose effect is dominant in the estimation errors of rotor position and speed.

As shown in(22), (24) and (25), the estimation error in rotor speed is proportional to the equivalent flux error, which is the main cause for incorrect estimation of rotor position and d-axis current. Since the actual rotor position is unknown, the error in d-axis current is used to compensate for the equivalent flux error based on disturbance theory.

$$\dot{\tilde{\psi}}'_{\mathrm{f}} = K_{\mathrm{e}}(i_{\mathrm{d}} - \hat{i}_{\mathrm{d}}) \tag{28}$$

Transforming (28) to αβ frame yields

$$\dot{\tilde{\psi}}'_{\mathrm{f}} = K_{\mathrm{e}}(\cos\hat{\theta}_{\mathrm{e}}(i_{\alpha} - \hat{i}_{\alpha}) + \sin\hat{\theta}_{\mathrm{e}}(i_{\beta} - \hat{i}_{\beta})) \tag{29}$$

$$\frac{d}{dt}\begin{pmatrix}\hat{i}_{\alpha}\\ \hat{i}_{\beta}\\ \hat{\omega}_{\mathrm{m}}\\ \hat{\theta}_{\mathrm{e}}\\ \hat{T}_{\mathrm{L}}\\ \tilde{\psi}'_{\mathrm{f}}\end{pmatrix} = \begin{pmatrix}\frac{-\hat{R}_{\mathrm{s}}}{\hat{L}_{\mathrm{q}}}\hat{i}_{\alpha} + \frac{\hat{\psi}_{\mathrm{syn}} + \tilde{\psi}'_{\mathrm{f}}}{\hat{L}_{\mathrm{q}}}P\hat{\omega}_{\mathrm{m}}\sin\hat{\theta}_{\mathrm{e}} + \frac{\upsilon'_{\alpha}}{\hat{L}_{\mathrm{q}}}\\ \frac{-\hat{R}_{\mathrm{s}}}{\hat{L}_{\mathrm{q}}}\hat{i}_{\beta} - \frac{\hat{\psi}_{\mathrm{syn}} + \tilde{\psi}'_{\mathrm{f}}}{\hat{L}_{\mathrm{q}}}P\hat{\omega}_{\mathrm{m}}\cos\hat{\theta}_{\mathrm{e}} + \frac{\upsilon'_{\beta}}{\hat{L}_{\mathrm{q}}}\\ \frac{1.5P\hat{\psi}_{\mathrm{syn}}i_{\mathrm{q}}}{J} - \frac{B}{J}\hat{\omega}_{\mathrm{m}} - \frac{\hat{T}_{\mathrm{L}}}{J}\\ P\hat{\omega}_{\mathrm{m}}\\ 0\\ 0\end{pmatrix} + \mathbf{K}'\begin{pmatrix}i_{\alpha} - \hat{i}_{\alpha}\\ i_{\beta} - \hat{i}_{\beta}\end{pmatrix} \tag{30}$$

where

$$\mathbf{K}' = \begin{pmatrix}K_{\mathrm{y}} & 0\\ 0 & K_{\mathrm{y}}\\ \frac{K_{\lambda}L_{\mathrm{q}}}{\psi_{\mathrm{syn}}}\sin\hat{\theta}_{\mathrm{e}} & -\frac{K_{\lambda}L_{\mathrm{q}}}{\psi_{\mathrm{syn}}}\cos\hat{\theta}_{\mathrm{e}}\\ \frac{K_{\lambda}L_{\mathrm{q}}}{P\hat{\omega}_{\mathrm{m}}\psi_{\mathrm{syn}}}\cos\hat{\theta}_{\mathrm{e}} & \frac{K_{\lambda}L_{\mathrm{q}}}{P\hat{\omega}_{\mathrm{m}}\psi_{\mathrm{syn}}}\sin\hat{\theta}_{\mathrm{e}}\\ -K_{\mathrm{t}}\sin\hat{\theta}_{\mathrm{e}} & K_{\mathrm{t}}\cos\hat{\theta}_{\mathrm{e}}\\ K_{\mathrm{e}}\cos\hat{\theta}_{\mathrm{e}} & K_{\mathrm{e}}\sin\hat{\theta}_{\mathrm{e}}\end{pmatrix}$$

The equivalent flux error is complemented in voltage equations of (18) to eliminate the steady state error in estimated rotor speed, and ultimately the estimation error in rotor position relating to $\tilde{\omega}_{\mathrm{m}}$. The extended nonlinear state observer with equivalent flux error compensation is shown in (30).

Simulation results in Fig. 4 show the performance of the extended nonlinear state observer against parameter inaccuracy with online compensation for equivalent flux error. Large steady state estimation errors shown in Fig. 3 are eliminated after the equivalent flux error is compensated. Nearly zero estimation error in rotor speed is obtained under steady state condition, while electrical angular position error is well below 2.5 degrees even in transient period. The remaining estimation error in rotor position is caused by $\tilde{L}_{\mathrm{q}}$ mainly, and could be further improved if an on-line inductance compensation method is supplemented.

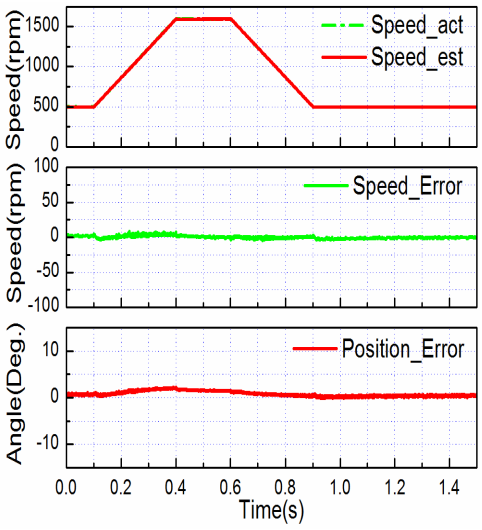

Fig. 4. Simulated performance of the extended nonlinear state observer against parameter inaccuracy with compensation for equivalent flux error.

4. Experimental Studies

The block diagram of the overall sensorless control system based on extended nonlinear state observer is shown in Fig. 5. Maximum Torque/Ampere control method is used to obtain current reference $\mathbf{i}^{*}_{\mathrm{dq}}$ in constant torque mode, while Optimal Field-Weakening control method is utilized in constant power mode [16]. An open-loop scheme is used to speed up the motor in start-up procedure. The specifications of the IPMSM used in simulation and experimental test are given in Table I.

Although the estimated speed is accurate under steady state condition, it suffers from poor dynamic performance due to the effects of stator resistance uncertainty, inaccurate

compensation for d- axis inductance, inverter nonlinearity and so on, especially in low speed range. So the average speed $\hat{\omega}_{avg}$, which is the derivative of the estimated rotor position, is used in the speed control system instead of the estimated speed directly obtained from the nonlinear state observer, as shown in Fig. 5. And a LPF (Low-Pass-Filter) is combined to get rid of the acoustic noise in the average speed, with cut-off frequency set at 200 Hz.

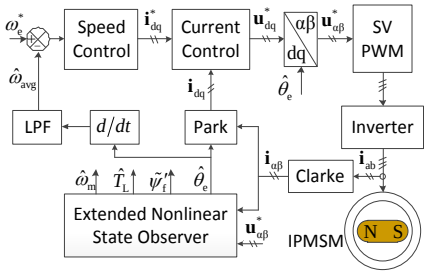

Fig. 5. Block diagram of the sensorless IPMSM speed control system

Table1. Specifications of IPMSM Simulation and Testing

Rated Power (kW)	1.0
Rated Current (A)	5.0
Rated DC Voltage (V)	310
PM flux linkage (Wb)	0.2
d- axis Inductance (mH)	13.0
q- axis Inductance (mH)	17.5
Stator resistance (Ω)	1.6
Pole Pairs	4
Rated Speed (rpm)	2000

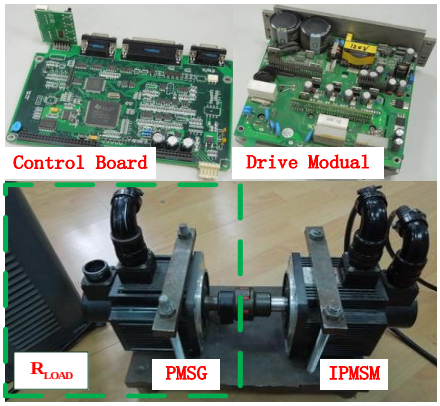

Fig. 6. Testing platform setup

The proposed extended nonlinear state observer is investigated on the testing platform shown in Fig 6. The control board is based on DSP TMS320F28234, with sampling frequency and PWM frequency both set to 10 kHz.

The DC bus voltage is measured, and reference voltage is fed to the extended nonlinear state observer instead of actual output voltage, along with dead time compensation using parameters available in datasheet [17-19]. Digital delay in SVPWM updating can be problematic in high speed range, and is well compensated in software by postponing the phase of reference voltage in αβ frame [9, 20].

Fig. 7 shows the performance of the proposed nonlinear state observer in experimental test. The IPMSM is controlled to accelerate from 500 rpm to 1600 rpm within 300 ms and vice versa. Although, accurate PM flux linkage and stator resistance are used in the extended state observer, steady state errors in the estimated rotor position and speed still exist due to the inverter nonlinearity, whose impact is more distinct in low speed range. Dynamic errors also arise in transient period duo to the lag in the estimated load torque, which is proportional to rotor speed.

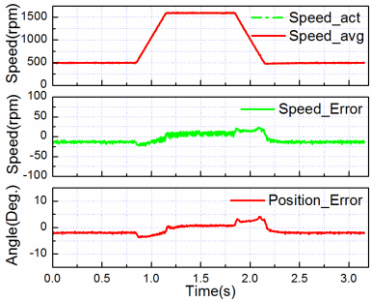

Fig. 7. Performance evaluation of the extended nonlinear state observer with accurate parameters.

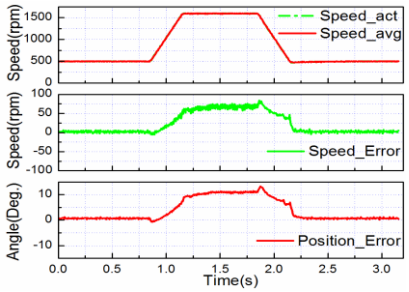

Fig. 8. Performance evaluation of the extended nonlinear state observer without compensation for equivalent flux error.

Fig. 8 and Fig. 9 illustrate the performance of the proposed extended nonlinear state observer with and without compensation for equivalent flux error. PM flux linkage in the observer is set to be 5% larger than its actual value deliberately, while other parameters are assumed to be approximately accurate. It should be noted that the average speed $\hat{\omega}_{avg}$ tracks the actual speed well in both cases.

Large steady state errors in the estimated rotor position and speed are observed in Fig. 8, owing to PM flux linkage inaccuracy and other non-idealities. The shape of the position estimation error is similar to that of the speed

estimation error, which demonstrates that the estimation error in rotor position caused by erroneously estimated speed is dominant.

These estimation errors caused by parameter inaccuracy, as well as inverter nonlinearity, are mitigated significantly when the equivalent flux error is on-line compensated using the method introduced in (28), as shown in Fig. 9. A very small zero steady state error in the estimated speed is obtained in both high and low speed region, while the overall electrical angular position error is limited within ± 5 degrees. It is worth noting that the equivalent flux error takes more time in low speed range to converge to its steady state value than that in high speed range, as the impact of PM flux linkage decreases with the decreasing rotor speed.

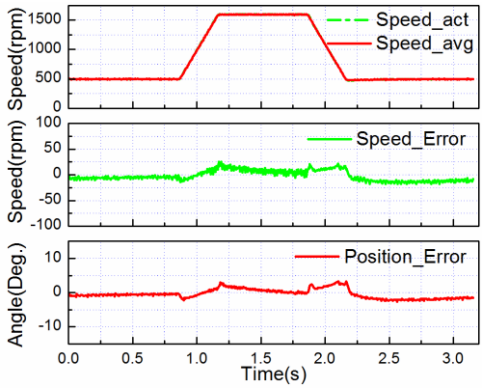

Fig.9. Performance evaluation of the extended nonlinear state observer with on line compensation for equivalent flux error.

5. Conclusion

In this paper, a novel extended nonlinear state observer for IPMSM is proposed based on a synthetic back EMF，along with the estimation of load torque. The impact of parameter uncertainty is investigated, and the steady state error equations are derived. It has been found that position estimation error caused by erroneously estimated speed is dominant in high speed range. The performance of the extended nonlinear state observer is improved significantly by incorporating on-line compensation for parameter errors, and the robustness against parameter inaccuracy, mainly the uncertainty of PM flux linkage, is enhanced

Acknowledgements

This work is supported by National Key Basic Research Program of China (2013CB035600) and Scientific Research Fund of Guangxi Provincial Education Department (2013YB143).

References

[1] G. C. Zhu, A. Kaddouri, L.-A. Dessaint, and O. Akhrif, “A nonlinear state observer for the sensorless control of a permanent-magnet AC machine,” IEEE Transactions on Industry Electronics, vol. 48, no. 6, pp. 1098–1108, Dec. 2001.

[2] J. Solsona, M. I. Valla, and C. Muravchik, “Nonlinear control of a permanent magnet synchronous motor with disturbance torque estimation,” IEEE Transactions on Energy Conversion, vol. 15, no. 2, pp. 163–168, Jun. 2000.

[3] G. Bisheimer, M. O. Sonnaillon, C. H. De Angelo, J. A. Solsona, G. O. Garcia, “Full speed range permanent magnet synchronous motor control without mechanical sensors,” IET Electric Power Applications, vol. 4, no. 1, pp. 35–44, 2010.

[4] B. S. Bhangu, C. M. Bingham, “GA-tuning of nonlinear observers for sensorless control of automotive power steering IPMSMs,” 2005 IEEE Conference on Vehicle Power and Propulsion, pp. 772–779.

[5] Z. Q. Chen, M. Doki, S. Tomita, S. Okuma, “An extended electromotive force model for sensorless control of interior permanent-magnet synchronous motors,” IEEE Transactions on Industry Electronics, vol. 50, no. 2, pp. 288–295, Apr. 2003.

[6] S. Koonlaboon, S. Sangwongwanich, “Sensorless control of interior permanent-magnet synchronous motors based on a fictitious permanent-magnet flux model,” Industry Applications Conference, Fourtieth IAS Annual Meeting, pp. 311–318, 2005.

[7] M. Hasegawa, S. Yoshioka, K. Matsui, “Position Sensorless Control of Interior Permanent Magnet Synchronous Motors Using Unknown Input Observer for High-Speed Drives,” IEEE Transactions on Industry Applications, vol. 45, no. 3, pp. 938–946, May/Jun. 2009.

[8] J. B. Liu, T. A. Nondahl, P. B. Schmidt, S. Royak, M. Harbaugh, “Rotor Position Estimation for Synchronous Machines Based on Equivalent EMF,” IEEE Transactions on Industry Applications, vol. 47, no. 3, pp. 1310–1318, May/Jun. 2011.

[9] Y. Park, S.-K. Sul, J.-K. Ji, Y.-J. Park, “Analysis of Estimation Errors in Rotor Position for a Sensorless Control System Using a PMSM,” Journal of Power

Electronics, vol. 12, no. 5, pp. 748–757, Sep. 2012.

[10] Y. SHI, K. Sun, M. Hongyan, L. Huang, Y. Li, "Permanent magnet flux identification of IPMSM based on EKF with speed sensorless control," 36th Annual Conference on IEEE Industrial Electronics Society, IECON 2010, pp. 2252–2257, Nov. 2010.

[11] S. Ichikawa, M. Tomita, S. Doki, S. Okuma, "Sensorless Control of Synchronous Reluctance Motors Based on Extended EMF Models Considering Magnetic Saturation With Online Parameter Identification," IEEE Transactions on Industry Applications, vol. 42, no. 5, pp. 1264–1274, Sep./Oct. 2006.

[12] S. Morimoto, M. Sanada, Y. Takeda, "Effects and Compensation of Magnetic Saturation in Flux-Weakening Controlled Permanent Magnet Synchronous Motor Drives," IEEE Transactions on Industry Applications, vol. 30, no. 6, pp. 1632–1637, Nov./Dec. 1994.

[13] K. Tatematsu, D. Hamada, K. Uchida, S. Wakao, T. Onuki, "Sensorless control for permanent magnet synchronous motor with reduced order observer," 29th Annual IEEE Power Electronics Specialists Conference, vol. 1, pp. 125–131, May. 1998.

[14] H. Matsuno, A. Moran, M. Hayase, "Design of controllers and observers for mimo nonlinear systems," Proceedings of the 35th SICE Annual Conference. International Session Papers, pp. 1059–1064, 1996.

[15] A. Isidori, Nonlinear Control Systems, 3rd ed., Springer-Verlag, 1995.

[16] Z. Q. Zhu, Y. S. Chen, D. Howe, "Online optimal flux-weakening control of permanent-magnet brushless AC drives," EEE Transactions on Industry Applications, vol. 36, no. 6, pp. 1661–1668, Nov./Dec. 2000.

[17] A. R. Munoz, T. A. Lipo, "On-line dead-time compensation technique for open-loop PWM-VSI drives," IEEE Transactions on Power Electronics, vol. 14, no. 4, pp. 683–689, Jul. 1999.

[18] J.-W. Choi, S.-K. Sul, "Inverter output voltage synthesis using novel dead time compensation," IEEE Transactions on Power Electronics, vol. 11, no. 2, pp. 221–227, Mar. 1996.

[19] D. Salt, D. Drury, D. Holliday, A. Griffo, P. Sangha, A. Dinu, "Compensation of inverter nonlinear distortion effects for signal injection based sensorless control," EEE Transactions on Industry Applications, vol. 47, no. 5, pp. 2084–2092, Sep./Oct. 2011.

[20] B.-H. Bae, S.-K. Sul, "A compensation method for time delay of full-digital synchronous frame current regulator of PWM AC drives," EEE Transactions on Industry Applications, vol. 39, no. 3, pp. 802–810, Nov./Dec. 2003

Yongle Mao received B.S and M.S degrees in electrical engineering from Harbin Institute of Technology, Harbin, China, in 2009 and 2011 respectively. He is currently working toward the Ph.D. degree in the College of Electrical Engineering, Zhejiang University, Zhejiang, China. His research interests are permanent magnet synchronous motor drives and sensorless control of AC machines.

Liu Guiying received the B.Eng. and M.Sc. degrees in electrical engineering from Zhejiang University, Hangzhou, China, in 1982 and 1989, respectively. She is currently with Guangxi Teachers Education University, Nanning, China. Her major research interests include the design and analysis of power electronics and renewable energy power conversion systems.

Chen Yangsheng received the B.S. degree and M.S. degree in college of electrical engineering from Zhejiang University, Zhejiang, China, and Ph.D. degree in department of electric and engineering from University of Sheffield, UK, in 1991 , 1994 and 1999, respectively. He was a principal engineer in CT and TRW, where he leaded many significant projects, including high power density motor for industrial robots, aero electrical drive system for flight control, development of servo motor for ABS/EPS/ABC system in automobile, research of ECU and sensors. He is currently a professor in college of electrical engineering, Zhejiang University. His research interests include permanent magnet synchronous control, application of power electronics, motor design for automobile and related control system, motor electromagnetism theory, research of motor vibration and noise.